

Site-response effects on RC buildings isolated by triple concave friction pendulum bearings

Sevket Ates*¹ and Muhammet Yurdaku²

¹Karadeniz Technical University, Department of Civil Engineering, Trabzon, Turkey

²Bayburt University, Department of Civil Engineering, Bayburt, Turkey

(Received December 23, 2010, Revised February 19, 2011, Accepted February 22, 2011)

Abstract. The main object of this study is to evaluate the seismic response effects on a reinforced concrete building isolated by triple concave friction pendulum (TCFP) bearings. The site-response effects arise from the difference in the local soil conditions at the support points of the buildings. The local soil conditions are, therefore, considered as soft, medium and firm; separately. The results on the responses of the isolated building are compared with those of the non-isolated. The building model used in the time history analysis, which is a two-dimensional and eight-storey reinforced concrete building with and without the seismic isolation bearings and/or the local soil conditions, is composed of two-dimensional moment resisting frames for superstructure and of plane elements featuring plane-stress for substructure. The TCFP bearings for isolating the building are modelled as of a series arrangement of the three single concave friction pendulum (SCFP) bearings. In order to investigate the efficiency of both the seismic isolation bearings and the site-response effects on the buildings, the time history analyses are elaborately conducted. It is noted that the site-response effects are important for the isolated building constructed on soft, medium or firm type local foundation soil. The results of the analysis demonstrate that the site-response has significant effects on the response values of the structure-seismic isolation-foundation soil system.

Keywords: seismic isolation; triple concave friction pendulum; gap elements; non-linear link element; site-response effects; series model; reinforced concrete building.

1. Introduction

While seismic isolation is increasingly applied to existing and new structures to reduce the seismic vulnerability, soil conditions has some adverse effects on the structures with and without seismic isolation systems during earthquakes. In order to overcome or reduce the harmful effects of soil conditions and earthquakes, seismic protection systems are, therefore, considered against these issues. Because of the development of numerical methods (Wong and Luco 1976, Idriss *et al.* 1979, Spyrakos and Beskos 1986, Gazetas 1991), many studies were done regarding the soil-structure interaction (SSI) effects (Wolf 1985, 1994; Goyal and Chopra 1989). The equations of motion of building systems with SSI were formulated for foundations comprising a joint mat or a set of individual spread footings by Novak and Henderson (1989). The influence of SSI and the possible effects of building and foundation rocking were examined by investigating the modal properties. Simplifications in the analysis were also suggested (Novak and Henderson 1989). Chaudhary *et al.* (2001) have identified

* Corresponding author, Assistant Professor, E-mail: sates@ktu.edu.tr

the structural and geotechnical parameters of four base-isolated bridges using available theoretical models and data from recent earthquakes. The main conclusions of their study are that the SSI effects depend primarily on horizontal pier stiffness in relation to the soil horizontal stiffness, and that the important reduction in the soil shear modulus for moderate earthquakes should be definitely incorporated into the SSI analyses. Vlassis and Spyarakos (2001) and Spyarakos and Vlassis (2002) performed analytical studies of the SSI effects on the longitudinal response of base-isolated bridge piers concerning the increase in damping and the decrease in base shear, as calculated by contemporary bridge design codes. They reached the conclusion that the SSI causes a significant decrease in the system. It is also well recognized that SSI has a significant role on structural response. However, common practice usually does not account for the effects of SSI on the seismic behaviour of base isolated structures. Cases in which the SSI needs to be incorporated in seismically isolated bridge design were identified and ways to take advantage of the SSI in order to enhance safety level and reduce design costs were recommended by Spyarakos and Vlassis (2002). The effects of the SSI on the peak responses of three-span continuous deck bridge seismically isolated with the elastomeric bearings were conducted by Tongaonkar and Jangid (2003). It was observed that the soil surrounding the pier has significant effects on the response of the isolated bridges and under certain circumstances the bearing displacements at abutment locations may be underestimated if the SSI effects are not considered in the response analysis of the system. Dicleli *et al.* (2005) studied the effect of the SSI effects on the seismic performance of seismic-isolated bridges. They reported that the analyses results revealed that SSI effects may be neglected in the seismic analysis of seismic-isolated bridges with heavy superstructure and light substructure constructed on stiff soil. However, the SSI effects need to be considered for bridges with light superstructure and heavy substructures regardless of the stiffness of the foundation soil. In soft soil conditions, soil-structure interaction effects need to be considered regardless of the bridge type. Soneji and Jangid (2008) studied the influence of the SSI on the behaviour of seismically isolated cable-stayed bridge supported on a rigidly capped vertical pile groups, which pass through moderately deep, layered soil overlying rigid bedrock. Spyarakos *et al.* (2009) studied quantify the effects of the SSI on seismically isolated building structures and reported that the SSI effects result in significant modifications on the structure-base isolation-foundation system frequency characteristics and are more significant for relatively stiff, squat structures founded on soft soil. Ates *et al.* (2009) studied earthquake response of isolated cable-stayed bridges under spatially varying ground motions. Tsai *et al.* (2010a and 2010b) conducted experimental and numerical studies for structures having sliding type isolators.

The all aforementioned studies were generally done for base isolated bridges and buildings having rubber or friction slider type bearings. However, the triple concave friction pendulum (TCFP) bearings newly developed have extensively not yet used in the analysis including the site-response effects. Hence, the aim of the present study is to highlight the effects of the site-response on seismically isolated building structures with the TCFP bearings. The GBZ000 component of 17 August 1999 Kocaeli Earthquake, Turkey, recorded at Gebze station available from PEER database is used as an earthquake record in the time history analysis.

The TCFP is consisted of two facing concave stainless steel surfaces and an articulated slider. The slider is separately placed between the two spherical stainless steel surfaces. In the system motions occur in sliding surfaces. The TCFP exhibits multiple changes in stiffness and damping properties during its motion. It is provided increasing amplitude of displacement. The great advantage of the TCFP bearing is that there is motion on two inner concave surfaces in small amplitude of earthquake while there is no motion on outermost surfaces. However, the motion occurs on the outermost

surfaces in case of more severe earthquake. Due to the fundamental law of the TCFP bearing, detritions do not occur on these surfaces and the system provides long living usage of these devices than the other sliding type isolation bearings. The principles of operation and force-displacement relationships of the TCFP bearings of different displacement capacities are developed by Fenz and Constantinou (2008a, 2008b). In these studies, it has been shown that when properly configured, these bearings provide stiffness and damping that change desirably with increasing displacement. Fadi and Constantinou (2010) reported that development of tools of simplified analysis and demonstration of their accuracy is required for the TCFP bearings. So, these tools are described and validation studies based on a large number of nonlinear response history analysis results are presented in the paper. It is shown that simplified methods of analysis systematically provide good and often conservative estimates of isolator displacement demands and good estimates of isolator peak velocities.

2. Modelling of the TCFP bearings

The TCFP bearing shown in Fig. 1 is consisted of two facing concave stainless steel surfaces coated with Teflon separated by a placed slider assembly. R_i is the radius of curvature of surface i , h_i is the radial distance between the pivot point and surface i and μ_i is the coefficient of friction at the sliding surface i , d_i is the displacement capacity of the surface i . Outer concave plates have effective radii $R_{eff1} = R_1 - h_1$ and $R_{eff4} = R_4 - h_4$. The articulated slider assembly consists of two concave plates separated by a rigid slider. Though the innermost slider is rigid, the assembly as a whole has the capability to rotate to accommodate differential rotations of the top and bottom plates. The friction coefficients on these concave plates are μ_1 and μ_4 . The inner concave plates have effective radii $R_{eff2} = R_2 - h_2$ and $R_{eff3} = R_3 - h_3$. Additionally, these surfaces are also coated with Teflon. The friction coefficients on these concave plates are μ_2 and μ_3 . This leads to motion of slider between up and down stainless of steel surfaces of slide plates. Unlike the SCFP and the double concave friction pendulum (DCFP), in the TCFP bearing there is no mechanical constraint defining which defined location of pivot point (Fenz and Constantinou 2008a, 200b).

Instead of this, pivot point corresponds to immediate centre of zero velocity of slider assembly. This centre is not a fixed point. It changes during sliding on the concave surfaces. Although, because the

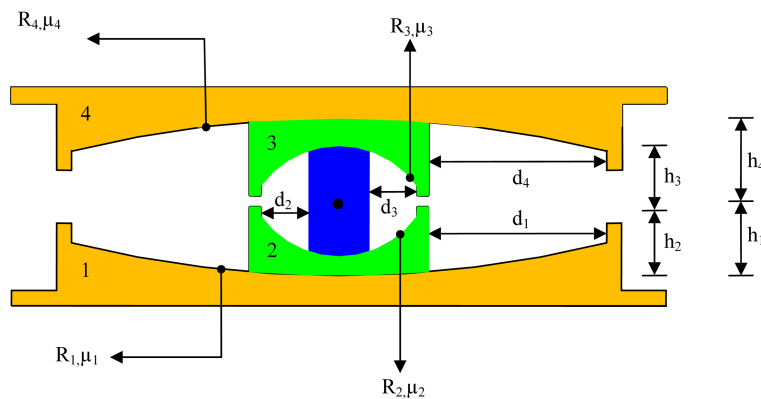


Fig. 1 The cross-section of the TCFP bearing and its definition of dimensions

immediate centre of zero velocity of up and down parts of the slider are always opposite directions, the immediate centre of velocity must always be between of them. In generally, the slider height is small than radii of curvature and there is little error occurred by assuming the immediate centre of velocity is fixed at middle of height of the articulated slider assembly. The DCFP and the TCFP bearings enable to simultaneously sliding on multiple concave plates. Hence it is constructed smaller than the SCFP bearing using the same general displacement capacity. In case economic benefits are taken into account, there is insignificant differentiation in the cost of the SCFP and the DCFP bearings of size. However, the TCFP bearing is cost effective as per bearing size and displacement capacity (Fenz 2008).

There are practicable no hysteresis rules or nonlinear elements present in structural analysis program that can be used to exactly model the TCFP bearing. For this reason, series model can be utilised in order to symbolize the TCFP bearing. The series model consists of nonlinear elements corresponding to the SCFP which can be used in present software structural analysis program. But, the TCFP bearing is not exactly like a model organized as a three SCFP bearing in series model although it is similar. Series models are favoured because of their implementation in available commercial structural analysis program such as SAP2000 (Computer and Structures 2007). It has nonlinear elements modelling rigid linear behaviour of the SCFP bearings. However, one behavioural event is preventing correctly modelling the TCFP bearing as a three SCFP bearing. This event is there is no sliding simultaneous on spherical concave surfaces 1 and 2. This observation is experimentally and analytically achieved by Fenz and Constantinou (2008c). At first, sliding occurs on spherical innermost concave surfaces 2 and 3 then stops when sliding starts on outermost spherical concave surfaces 1 and 4. Then sliding starts on innermost surfaces 2 and 3 again when the outer concave plates contacts restrainers' displacement. The mentioned possible positions of the motion are depicted in Fig. 2.

The three SCFP bearing elements are connected to each other in series to represent the TCFP bearing. The model is called series model. In this model, $1/\bar{R}_{effi}$, $\bar{\mu}_i$ and \bar{d}_i represent the stiffness of the spring based on the effective radius of curvature i ; the velocity dependent coefficient of friction and the displacement of the gap link element, respectively. Over bar notation is employed to symbolize parameters and responses related with the series model. In the other hand, normal notation is employed to symbolize parameters and responses related with the TCFP bearing. In the series model, displacement of element i begins when horizontal force, F , exceeds the friction force. The friction force for each concave surface by means of $\bar{F}_{fi} = \bar{\mu}_i W$ where W is the vertical load acting on the bearing. Motion of i elements stop when i_{th} element displacement becomes equal to displacement capacity \bar{d}_i . This occurs at an applied horizontal force of

$$F_i = \frac{W}{\bar{R}_{effi}} \bar{d}_i + \bar{\mu}_i W \quad (1)$$

The force-displacement relationship can be obtained by considering the series model is depicted in

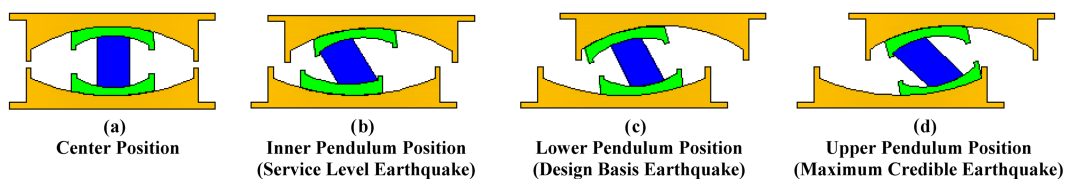


Fig. 2 The possible positions of the TCFP bearing

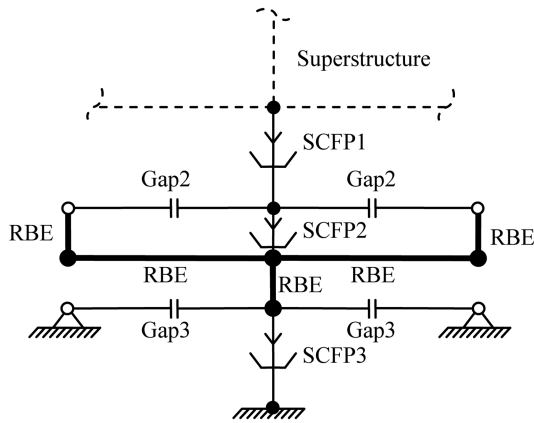


Fig. 3 Series model of the TCFP bearing used in SAP2000 for the building excluding foundation soil

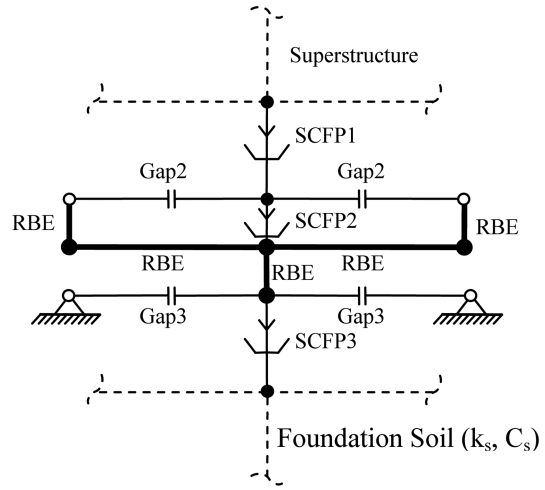


Fig. 4 Series model of the TCFP bearing used in SAP2000 for the building including foundation soil

Fig. 4. The model nearly gives the same actual force-displacement relationship which exhibits the TCFP bearing. The series model is recommended by Fenz and Constantinou (2008c). Figs. 3 and 4 show how to create the series model of the TCFP bearing in SAP2000 (Computer and Structures 2007) is by assembling of the three single concave friction pendulum (SCFP) link elements, four gap link elements, and five rigid beam elements (RBE).

4. Formulation for the series model of the TCFP

In the series modelling scheme proposed by Fenz and Constantinou (2008c), the SCFP1 link element represents the combined behaviour of inner surfaces 2 and 3, the SCFP2 link element represents the behaviour of outer surface 1 and the SCFP3 link represents outer surface 4. Since there is no adjustment made to the vertical load supported by the bearings, to ensure that sliding initiates correctly for each element there are no modifications made to the coefficients of friction. That is

$$\bar{\mu}_1 = \mu_2 = \mu_3 \tag{2}$$

$$\bar{\mu}_2 = \mu_1 \tag{3}$$

$$\bar{\mu}_3 = \mu_4 \tag{4}$$

The actual behaviour is sliding occurring only on surfaces 2 and 3. In the series model, sliding takes place only for FP1 link element. And so, it is essential that

$$\bar{R}_{eff1} = R_{eff2} + R_{eff3} \tag{5}$$

The effective radius of the SCFP2 link element in the series model is obtained by equating the stiffness given by the series model with the actual stiffness exhibited by the bearing

$$\frac{W}{\bar{R}_{eff1} + \bar{R}_{eff2}} = \frac{W}{R_{eff1} + R_{eff3}} \quad (6)$$

and combining Eqs. (5) and (6), the effective radius for the SCFP2 link element can be obtained as

$$\bar{R}_{eff2} = R_{eff1} - R_{eff2} \quad (7)$$

In a similar way, the effective radius of the SCFP3 link element in the series model is attained by equating the stiffness given by the series model with the actual stiffness exhibited by the bearing

$$\frac{W}{\bar{R}_{eff1} + \bar{R}_{eff2} + \bar{R}_{eff3}} = \frac{W}{R_{eff1} + R_{eff4}} \quad (8)$$

by combining Eqs. (5), (7) and (8), the effective radius for the SCFP3 link element can be obtained as

$$\bar{R}_{eff3} = R_{eff4} - R_{eff3} \quad (9)$$

In the series model, gap link elements are also used in order to achieve the true force-displacement relationship of the TCFP bearing. The displacement of the gap link elements are given by following equations

$$\bar{d}_2 = \frac{R_{eff1} - R_{eff2}}{R_{eff1}} d_1 \quad (10)$$

$$\bar{d}_3 = \frac{R_{eff4} - R_{eff3}}{R_{eff4}} d_4 \quad (11)$$

If desired to model the total displacement capacity of the bearing, the displacement capacity of the SCFP1 link element can be assigned as

$$\bar{d}_1 = (d_1 + d_2 + d_3 + d_4) - (\bar{d}_2 + \bar{d}_3) \quad (12)$$

The rate parameter, a , is adjusted to properly model the velocity dependence of the coefficient of friction on outer surfaces 1 and 4. This is provided by indicating

$$\bar{a}_2 = \frac{R_{eff1}}{R_{eff1} - R_{eff2}} a_1 \quad (13)$$

$$\bar{a}_3 = \frac{R_{eff4}}{R_{eff4} - R_{eff3}} a_4 \quad (14)$$

For the SCFP1 link element of the series model, the rate parameter can be specified as half of the average of the rate parameters on surfaces 2 and 3 of the TCFP bearing. Therefore

$$\bar{a}_1 = \frac{a_2 + a_3}{4} \quad (15)$$

5. Time history analysis in SAP2000

The method of time history analysis used in this study is an extension of the Fast Nonlinear Analysis method developed by Ibrahimbegavich and Wilson (1989), and Wilson (1993). The method extremely efficient and is designed to be used for structural systems which are linear elastic, but

which have nonlinear link elements. The dynamic equilibrium equation of a linear structure having nonlinear link elements subjected to an earthquake load can be written as

$$\mathbf{K}_L u(t) + \mathbf{C} \dot{u}(t) + \mathbf{M} \ddot{u}(t) + \mathbf{r}_N(t) = \ddot{\mathbf{U}}_g(t) \tag{16}$$

where \mathbf{K}_L is the stiffness matrix of the linear elastic elements; \mathbf{C} is the damping matrix; \mathbf{M} is the diagonal mass matrix; \mathbf{r}_N is the vector of forces from the nonlinear degrees of freedom in the nonlinear link elements such as gap element and link element corresponding to single concave friction pendulum; $\mathbf{u}, \dot{\mathbf{u}}$ and $\ddot{\mathbf{u}}$ are the relative displacements, velocities, and accelerations with respect to ground; and $\ddot{\mathbf{U}}_g$ is the vector of applied earthquake load. All nonlinear link elements are needed to be defined as linear effective stiffness for each degree of freedom of the nonlinear link elements. The equilibrium equation can then be rewritten as

$$\mathbf{K} u(t) + \mathbf{C} \dot{u}(t) + \mathbf{M} \ddot{u}(t) = \ddot{\mathbf{U}}_g(t) - [\mathbf{r}_N(t) - \mathbf{K}_N u(t)] \tag{17}$$

in which $\mathbf{K} = \mathbf{K}_L + \mathbf{K}_N$ with \mathbf{K}_L being the stiffness of all the linear elements and for linear degrees of freedom of nonlinear link elements, and \mathbf{K}_N being the linear effective-stiffness matrix for all the nonlinear degrees of freedom.

6. Numerical example

The time history analysis of the isolated and non-isolated reinforced concrete building structure is examined including site-response effects. A two-dimensional and eight story-building structure is selected as a model in order to execute the analyses. The TCFP bearings are selected for the isolation devices and placed between the bottom of the columns and the foundations. The TCFP bearings are modelled as the series model of the TCFP bearing in SAP2000 (Computer and

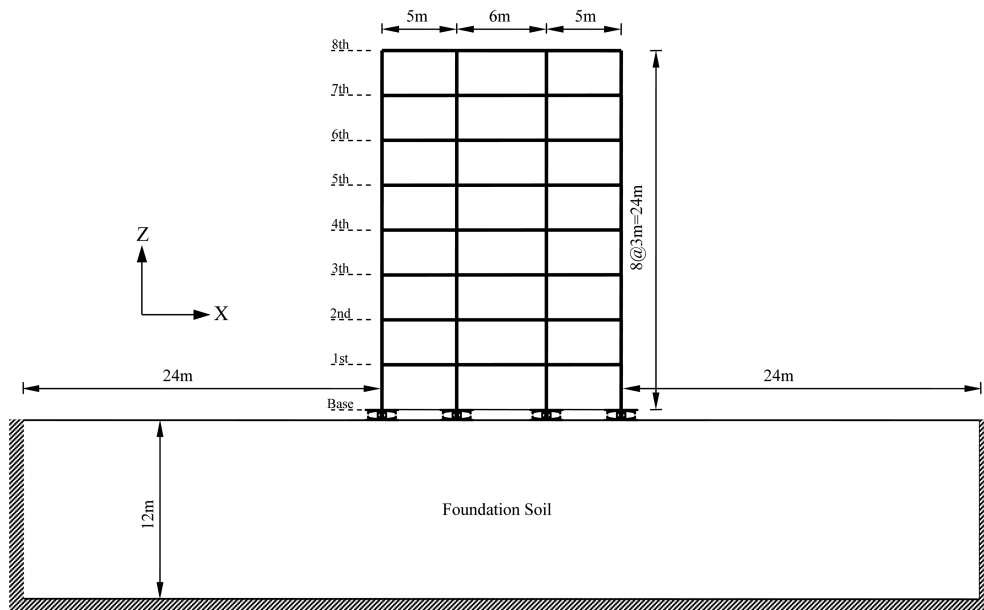


Fig. 5 Two-dimensional model of the structure considering foundation soil

Table 1 Cross-sectional properties of the building

Section name	Cross-section (cm/cm)	Inertia moment (10^{-3} m^4)	Unit volume weight (kN/m^3)	Modulus of elasticity (MPa)
Columns	30/80 (1 st to 2 nd stories)	12.800	25	28000
	30/70 (3 th to 5 th stories)	8.575		
	30/50 (6 th to 8 th stories)	3.125		
Beams	30/60	5.400	25	28000

Table 2 Actual properties of the TCFP bearing

Name of property	Value
$R_{eff1} = R_{eff4}$ (mm)	1200
$R_{eff2} = R_{eff3}$ (mm)	230
$d_1 = d_4$ (mm)	200
$d_2 = d_3$ (mm)	80
$\mu_1 = \mu_4$	0.040
$\mu_2 = \mu_3$	0.010

Structures 2007) by assembling of three friction pendulum (FP) link elements, four gap link elements and five rigid beam elements (RBE). A schematic model of the structure mentioned above is shown in Fig. 5. The cross sectional properties of the column and beam elements of the structure are given in Table 1. Damping ratio is specified as 5% for reinforced concrete building. Effective radius of curvature, frictional properties and displacement capacities of the TCFP bearings are given in Table 2. The parameters related to the TCFP bearings used in the analysis can be selected in accordance with the design basis and maximum credible earthquakes which may occur at the site where the structure is constructed. The masses due to gravity loads of the beams, the columns, and the slabs and live and death loads on the slabs are considered as lumped masses at the connection joints of the beams and the columns.

The foundation soil is assumed to be linearly elastic and represented by four-node plane elements up to a certain distance from the building. To avoid reflection of the outgoing waves, these plane elements are assumed to be massless (Leger and Boughoufalah 1989, Akkose *et al.* 2008). The properties of the foundation soil are given in Table 3 (Soneji and Jangid 2008). The 768 plane elements featuring plane-stress are used in the finite element mesh of the foundation soil.

Input parameters in series model, which are calculated by using values of Table 2 and Eqs. (5) to (15), are given in Table 4 in which SCFP1 link element represents inner surfaces 2 and 3, FP2 link element represents outer surface 1, and SCFP3 link element represents outer surface 4. Sum of the

Table 3 Foundation soil properties

Soil type	Poisson's ratio (unitless)	Unit volume weight (kN/m^3)	Modulus of shear (kN/m^2)	Modulus of elasticity (kN/m^2)	Damping ratio C_s (%)
Soft	0.40	20	245000	686000	0.06
Medium	0.35	22	1225000	3308000	0.04
Firm	0.30	24	2250000	5850000	0.02

Table 4 Parameters of the series model of the TCFP bearing used in the analysis

FP link element	Friction Coefficient $\bar{\mu}_i$	Radii of curvature R_{effi} (mm)	Elastic stiffness K_i (kN/m)	Rate parameter \bar{a}_i (sec/mm)	Gap displacement \bar{d}_i (mm)
FP1 ($i=1$)	0.010	460	8500	0.050	
FP2 ($i=2$)	0.040	970	34000	0.124	162
FP3 ($i=3$)	0.040	970	34000	0.124	162

Properties of the series model for analysis in SAP2000

element heights are equal to actual TCFP bearing. Shear deformation occurs at the semi-height of the element. It can be said that the link element mass does not affect the result of the analysis. However, it is necessary for efficiency of the analysis.

To properly represent the vertical stiffness of the bearing, the modulus of elasticity of the bearing is specified to be related with that of the steel. The bearing is not exactly a solid piece of metal so that the modulus is reduced to half to approximate the actual situation. So, the modulus of elasticity of the bearings is taken as $E = 1.05 \times 10^8$ kN/m² (Constantinou *et al.* 2007). Hence, the vertical stiffness of the bearing is

$$K_v = \frac{EA}{h} \tag{18}$$

where A is the area of the slider and h is the real height of the bearing. Elastic stiffness is, furthermore, equal to

$$K = \frac{\bar{\mu}_i W}{2D_Y} \tag{19}$$

in which $\bar{\mu}_i$ is coefficient of friction on the surface i for high speed motion; W is axial load supported by the bearing and D_Y denotes yield displacement and is taken as 1 mm. Effective stiffness is equal to

$$K_{effi} = \frac{W}{R_{effi}} \tag{20}$$

where \bar{R}_{effi} is i th element of the effective radius. Besides, rate parameter is coefficient dependent velocities which provide transition between maximum and minimum value of coefficient of friction, and is taken as to be 0.1 sec/mm for each actual sliding surfaces 1 to 4. By means of Eqs. (18) to (20), the properties of the SCFP link element utilized in SAP2000 (Computer and Structures 2007) is summarized in Table 5. Herein, the friction coefficient-slow stands for the half of the friction coefficient-fast at the high speed motion.

Unidirectional excitation along the axis X of the building is applied using the GBZ000 component of 17 August 1999 Kocaeli earthquake recorded at Gebze station in Fig. 6. The peak acceleration and displacement of the ground motion are 0.244 g and 424.70 mm, respectively. The motion is scaled by a factor of 2 in order to show all possible sliding positions mentioned in Fig. 2 of the TCFP bearings. The acceleration of gravity is also included in the vertical component by using a ramp function in the beginning of the time history in order to take into account the effect of the dead load on the behaviour of the TCFP bearings. The TCFP bearing is modelled using the SCFP and the gap link elements having nonlinear properties. The time history analysis is carried out for

Table 5 Properties of the FP link elements used in SAP2000

	FP1	FP2	FP3
Element height (mm)	100	50	100
Shear deformation location (mm)	50	25	50
Supported weight (kN)	1700	1700	1700
Vertical stiffness (kN/m)	4174882	4174882	4174882
Elastic stiffness (kN/m)	8500	34000	34000
Effective stiffness (kN/m)	3696	1753	1753
Friction coefficient-fast	0.010	0.040	0.040
Friction coefficient-slow	0.005	0.020	0.020
Radius (mm)	460	970	970
Rate parameter (sec/mm)	0.050	0.124	0.124

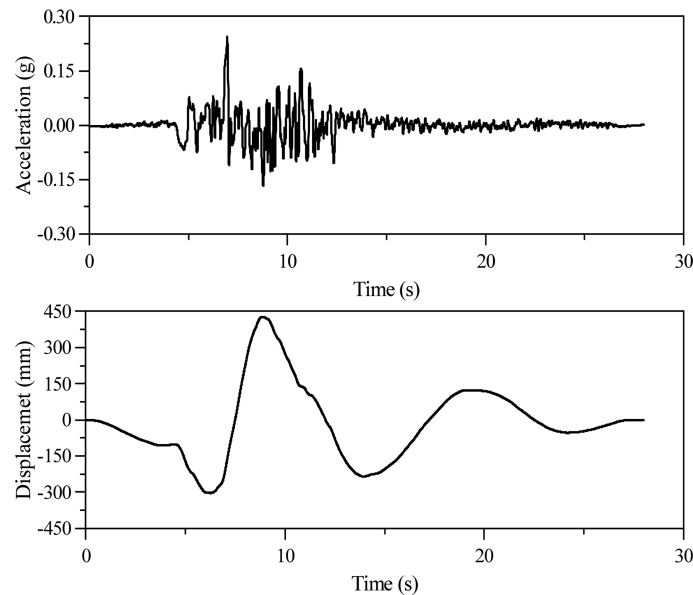


Fig. 6 Ground acceleration and displacement histories of the 1999 Kocaeli earthquake recorded at Gebze station

the isolated and the non-isolated buildings. The first five periods of vibration of the isolated and non-isolated buildings with and without the site-response effects determined from the analysis are given in Table 6. It is clearly seen that the dominant periods of the non-isolated without the site-response effects are smaller than these of the non-isolated building including the site-response effects. When the site-response is considered, the period of the non-isolated building constructed on firm soil is smallest. The periods of the isolated building founded on soft, medium or firm foundation soil are nearly closed to each other. However, the foundation soil is getting stiffer, the periods decrease. So, the periods of the non-isolated building constructed on firm soil condition trends to approach those of the non-isolated building excluding the site-response effects. The dominant period of the ground motion is 0.400 sec. Inclusion of the site-response effect, it may be said that the resonance risk is increase at the second mode for the structure with and without base isolation constructed on

Table 6 Periods for the isolated and non-isolated buildings

Mode No	Without site-response		With site-response					
	Isolated	Non-isolated	Isolated			Non-isolated		
			Period (sec)			Period (sec)		
Period (sec)	Soft soil	Medium soil	Firm soil	Soft soil	Medium soil	Firm soil		
1	3.219	0.885	3.262	3.241	3.243	1.140	1.073	1.065
2	0.482	0.306	0.412	0.387	0.383	0.363	0.356	0.356
3	0.228	0.169	0.190	0.158	0.158	0.194	0.191	0.191
4	0.159	0.119	0.158	0.157	0.157	0.194	0.129	0.129
5	0.158	0.106	0.158	0.139	0.131	0.157	0.128	0.118

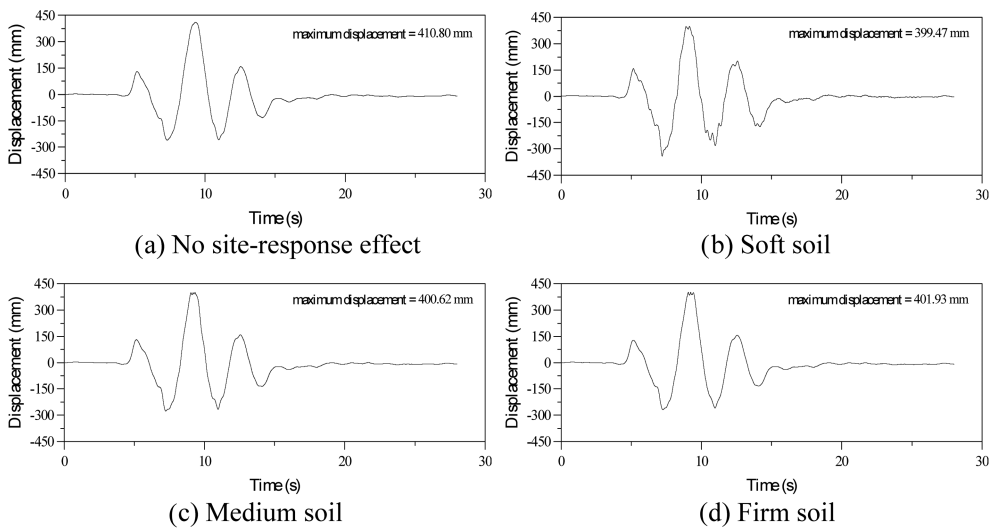


Fig. 7 Displacement histories of the TCFP bearing for different soil conditions

all type soil considered.

Isolator displacement obtained from analysis with and without site-response effects is depicted in Fig. 7 for the isolated building founded on the soft, medium and firm soil. It is seen from the figure that maximum displacement reaches to 410.80 mm for isolated building without site-response. When the soil structure interaction is considered, the maximum displacement at the TCFP bearing is obtained as 399.47 mm, 400.62 mm and 401.93 mm for the isolated building founded on the soft, medium and firm soil, separately. It can be said that the interaction is not important for estimation of the displacement capacities of the TCFP bearings. The capacities does not also exceed if the isolated is constructed on having different stiffness of the foundation soils. Displacement capacity of the TCFP bearings is expected as 413.80 mm. The value of capacity is viable for soft, medium and firm foundation soil. The peak displacement of the earthquake ground motion as mentioned above is 424.70 mm. This value shows that the motion firstly starts inner surfaces 2 and 3 only. At the position of the bearing uses own approximately 13.80 mm displacement capacity given by Eqs. (19) and (20) when the forces acting on the surfaces 2 and 3 are up to value of 68 kN calculated by the Eqs. (23) and (24). Then the motion stops on surface 2 and sliding occurs on surfaces 1 and 3 as

long as friction forces are to be between 68 kN and 351.33 kN calculated by the Eqs. (25) and (26); this time the bearing may approach totally 413.80 mm-displacement capacity given by Eq. (21). Afterwards the friction forces exceed to 351.33kN, the displacement of the TCFP bearing goes to maximum values of 413.80 mm. Because the motions on the sliding surfaces 1-4 are based on the friction forces occurring on the sliding surfaces and the radii of the curvature of the surfaces. That is why; the possible positions of the TCFP bearings are not change by changing the type of the foundation soils.

$$u_I = (\mu_1 - \mu_2)R_{eff2} + (\mu_1 - \mu_3)R_{eff3} \quad (21)$$

$$u_{II} = u_I + (\mu_4 - \mu_1)(R_{eff1} + R_{eff3}) \quad (22)$$

$$u_{III} = u_{II} + \left(1 + \frac{R_{eff4}}{R_{eff1}}\right)d_1 - (\mu_4 - \mu_1)(R_{eff1} + R_{eff4}) \quad (23)$$

$$u_{IV} = u_{III} + \left[\left(\frac{d_4}{R_{eff4}} + \mu_4\right) - \left(\frac{d_1}{R_{eff1}} + \mu_1\right)\right](R_{eff2} + R_{eff4}) \quad (24)$$

$$u_V = d_1 + d_2 + d_3 + d_4 \quad (25)$$

where u_I , u_{II} , u_{III} , u_{IV} and u_V are the displacements occurring on the surfaces at the different possible positions of the motion. The position I of the TCFP bearings is that the sliding begins on the surface 2 and 3 only, and no sliding on surface 1 and 4. The position II is the motion stops on the surface 2 and sliding occurs on surface 1 and 3. In case of the position III, the motion stopped on the surface 2 and 3; sliding initiates on the surfaces 1 and 4. At the position IV, slider contacts restrainer on the surface 1 and the motion remains stopped on the surface 3, then sliding on the surfaces 2 and 4. The last position V is that slider bears on restrainer of the surface 1 and 4; sliding occurs on the surfaces 2 and 3. The displacement capacities of the each possible position corresponds to Eqs. (21) to (25). The other parameters are defined beforehand. Base shear forces for the isolated and non-isolated building are also plotted in Figs. 8 and 9 for the three cases of the

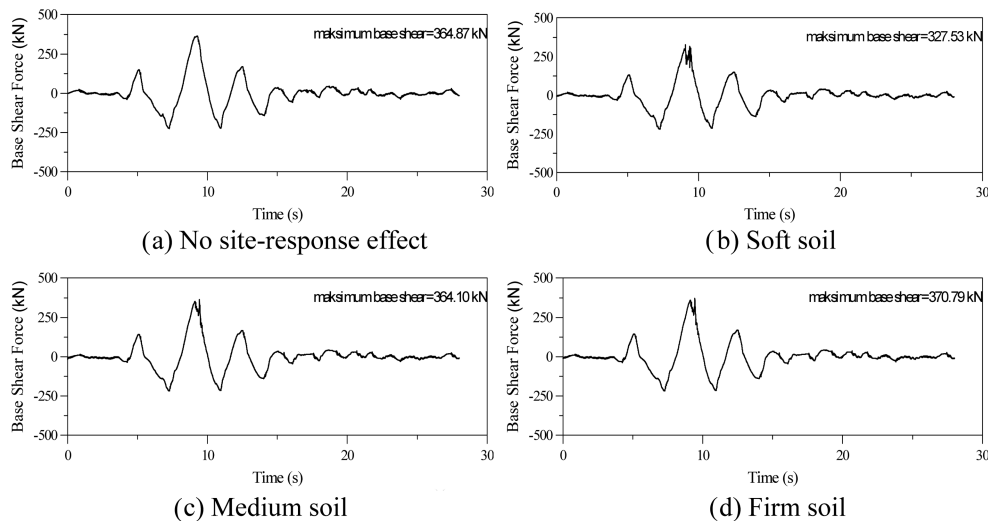


Fig. 8 Base shear force histories of the isolated buildings for different soil conditions

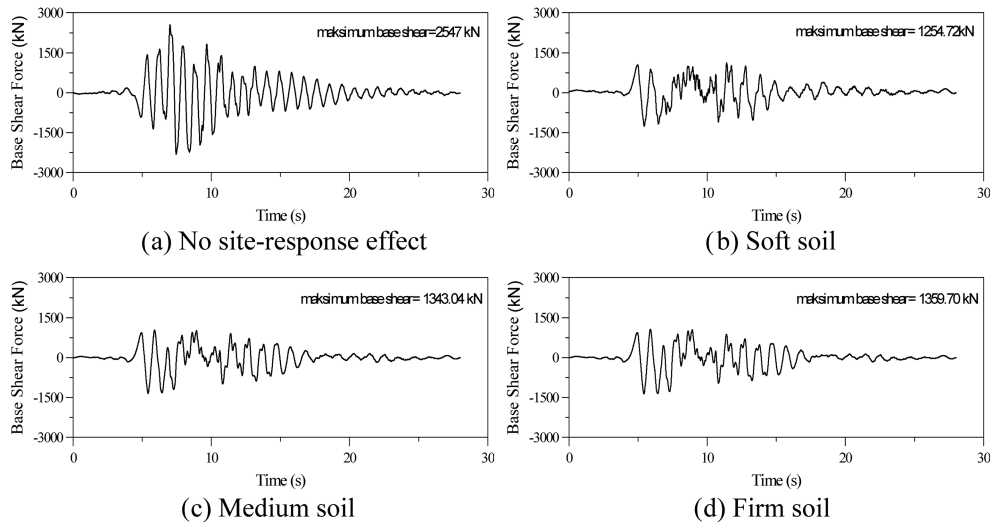


Fig. 9 Base shear force histories of the non-isolated buildings for different soil conditions

foundation soil. In case the site-response effects are not considered, the base shear force at the bearing level is approximately obtained as $0.215W$ for the isolated building while the base shear force is $0.456W$ for the non-isolated building. The maximum values of the base shear forces for the isolated and non-isolated cases are 364.87 kN and 808.74 kN , respectively. Provide that the site-response effects are included in the analysis for the isolated and non-isolated building, the base shear forces are acquired as $0.193W$, $0.214W$ and $0.218W$ for soft, medium and firm foundation soil conditions, respectively. In the event of the medium foundation soil; the base shear force is nearly closed to that of the building excluding the site-response effects. The Fig. 8 shows that the isolation bearing significantly reduces the base shear forces at the all cases. Additionally, shear force-displacement relationship at the TCFP bearing level is given in Figs. 10-13. The behaviour of the loop described as hysteretic. The energy dissipated per cycle is equal to the area under the loop. Owing to the area, the effective damping of the bearing can be calculated on an average. The figures related to loops have nearly the same area corresponding to dissipated energy of the TCFP bearings.

$$F_I = \mu_1 W \tag{25}$$

$$F_{II} = \mu_4 W \tag{26}$$

$$F_{III} = \frac{W}{R_{eff1}} d_1 + \mu_1 W \tag{27}$$

$$F_{IV} = \frac{W}{R_{eff4}} d_4 + \mu_4 W \tag{28}$$

$$F_V = \frac{W}{R_{eff2} + R_{eff3}} (u_V - u_{IV}) + \frac{W}{R_{eff4}} d_4 + \mu_4 W \tag{29}$$

where F_I , F_{II} , F_{III} , F_{IV} and F_V are the shear forces occurring on the surfaces at the different possible positions of the motion.

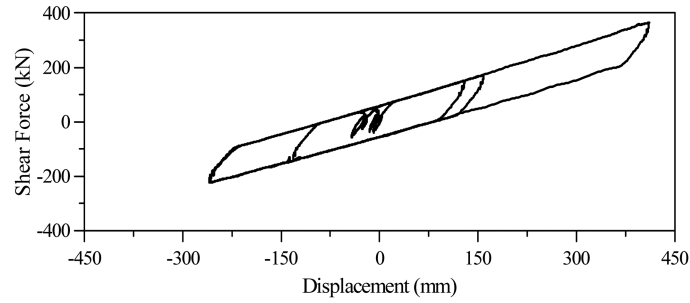


Fig. 10 Shear force-displacement loop at the TCFP bearing for the isolated building without SSI

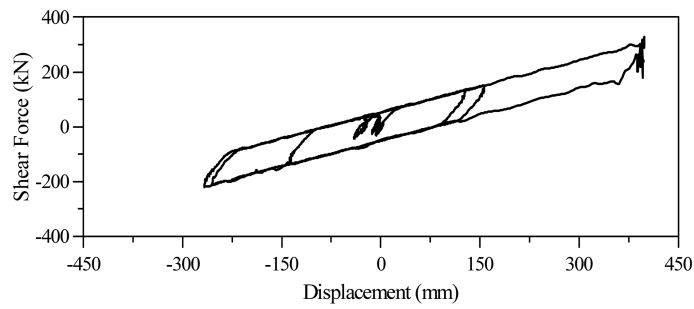


Fig. 11 Shear force-displacement loop at the TCFP bearing for the isolated building founded on soft foundation soil

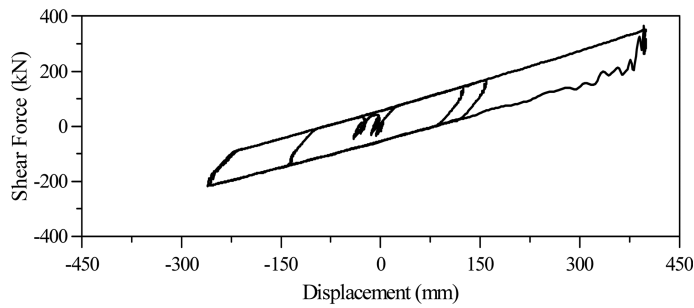


Fig. 12 Shear force-displacement loop at the TCFP bearing for the isolated building founded on medium foundation soil

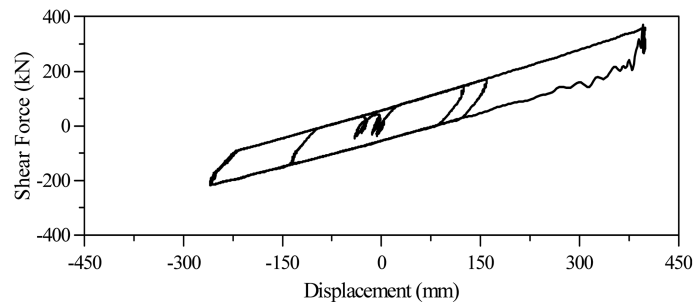


Fig. 13 Shear force-displacement loop at the TCFP bearing for the isolated building founded on firm foundation soil

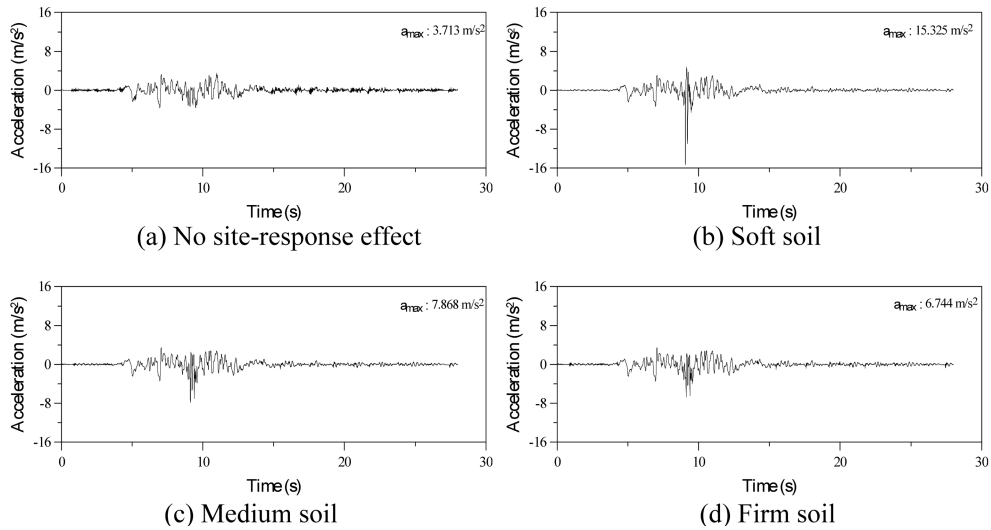


Fig. 14 First floor acceleration histories of the isolated buildings

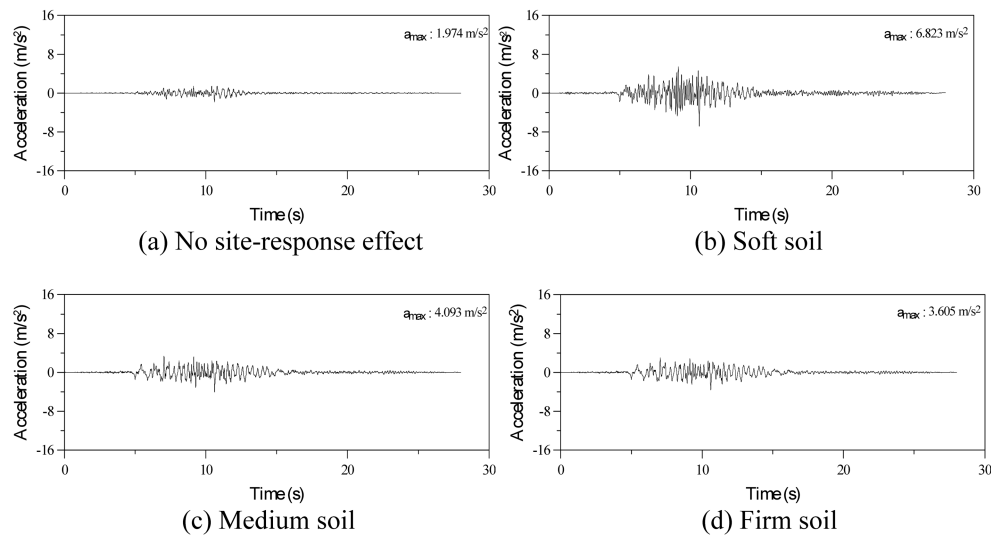


Fig. 15 First floor acceleration histories of the non-isolated buildings

Figs. 14 to 19 give an opportunity to compare the structural accelerations at the first, fourth and top floor levels. The building constructed on the soft foundation soil is more sensitive to ground acceleration as compared to medium and firm foundation soil cases. The results are viable for both the isolated and the non-isolated buildings. However, the accelerations transmitted to the building scale down by means of using the isolation technique when the accelerations increase throughout the floor levels of the non-isolated building. Hence, the usage of the TCFP bearing to seismically isolate building can be suggested.

The inter-story displacements of the considered building are presented in Table 7. The table demonstrates that relative displacements at the each floor of the isolated building with the TCFP bearings are significantly smaller than these of the non-isolated building. On the other hand, the

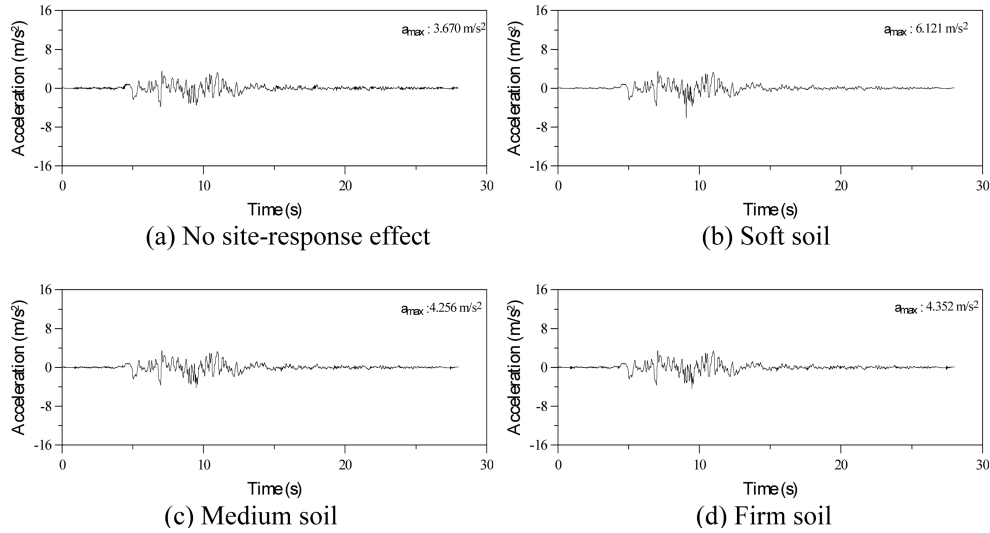


Fig. 16 Fourth floor acceleration histories of the isolated buildings

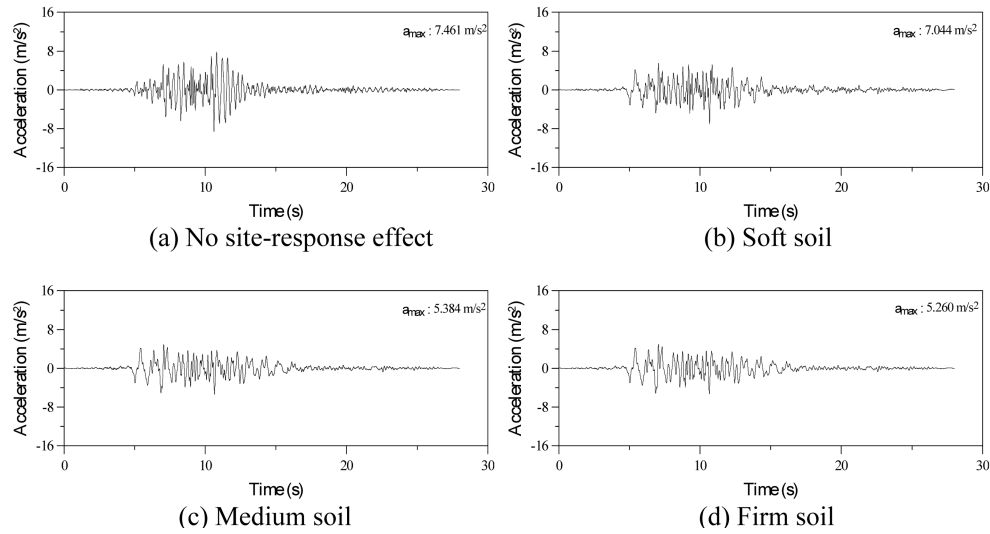


Fig. 17 Fourth floor acceleration histories of the non-isolated buildings

floor displacements of the non-isolated building increase when as ranging from the first to top floor levels. On the other hand, the maximum relative displacements of the isolated building obtained from the nonlinear time history analysis are smaller as compared to these of the non-isolated building.

As a result of decreasing of the relative displacements at the floor level of the seismically isolated building, inertia forces developed on the columns and beams elements of the building under the consideration such as bending moment, shear and axial forces may decrease shown in the following figures 20 to 25. All inertia forces of the non-isolated building with or without the site-response effects are larger than these of the isolated building. Shear forces of the isolated building including

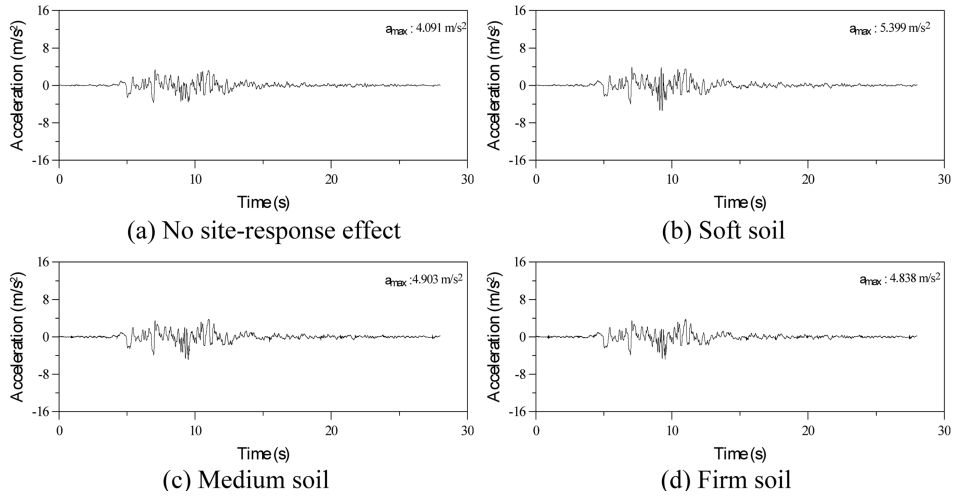


Fig. 18 Top floor acceleration histories of the isolated buildings

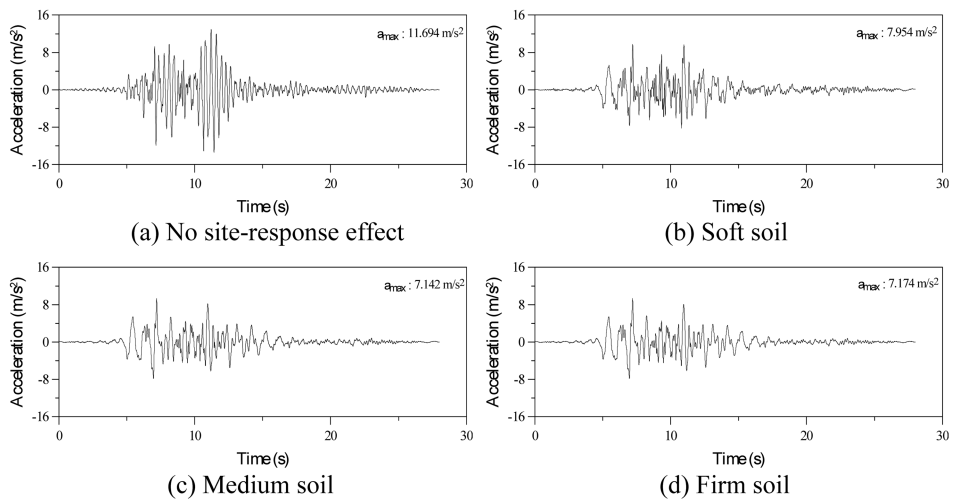


Fig. 19 Top floor acceleration histories of the non-isolated buildings

Table 7 Maximum inter-story displacement (mm)

Storey No	Non-Isolated			Isolated		
	Foundation soil conditions			Foundation soil conditions		
	Soft	Medium	Firm	Soft	Medium	Firm
1	27.40	26.48	26.32	12.33	11.00	9.54
2	45.93	44.64	44.38	26.53	23.48	21.93
3	62.64	60.95	60.59	40.43	35.88	34.17
4	77.46	75.16	74.70	52.68	47.02	45.17
5	90.61	87.37	86.77	63.33	56.38	54.37
6	104.40	100.00	99.27	74.33	65.78	63.37
7	114.50	108.70	111.20	82.43	72.48	70.07
8	120.94	114.60	119.49	88.31	76.62	74.06

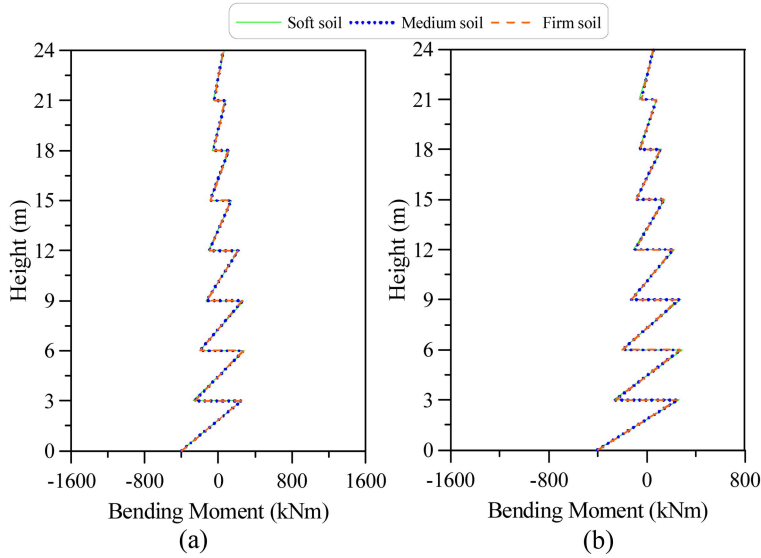


Fig. 20 The site-response effects on the bending moment distribution throughout the height of (a) the isolated and (b) the non-isolated buildings

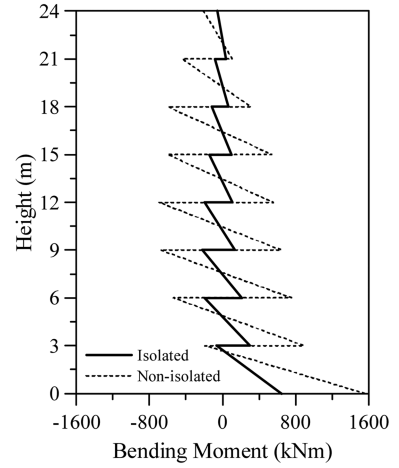


Fig. 21 Bending moment distribution throughout the height of the isolated and non-isolated buildings without the site-response effects

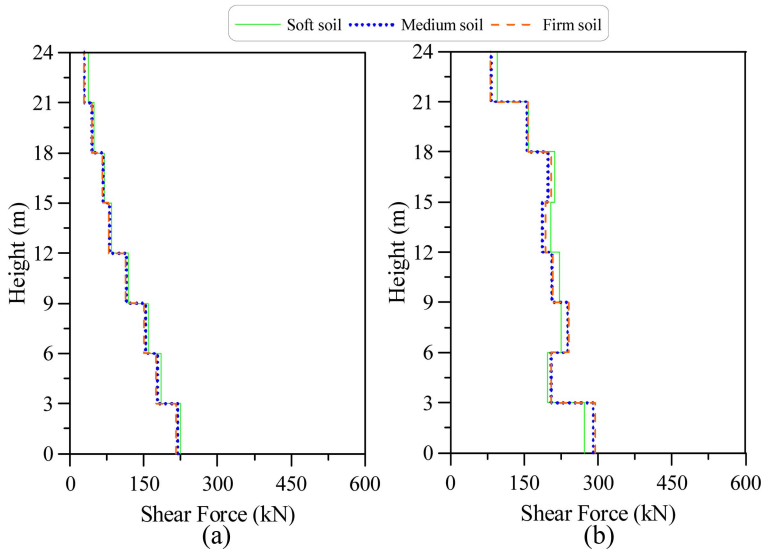


Fig. 22 The site-response effects on the shear force distribution throughout the height of (a) the isolated and (b) the non-isolated buildings

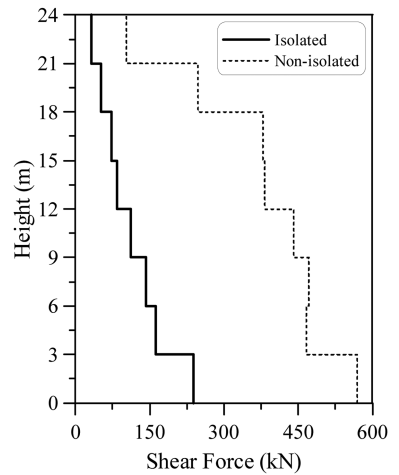


Fig. 23 Shear force distribution throughout the height of the isolated and non-isolated buildings without the site-response effects

the site-response effects decrease while the bending moment and axial force are nearly the same as compared to those of the isolated building excluding site-response effects. All inertia forces of the non-isolated building including site-response effects decrease while those of the non-isolated

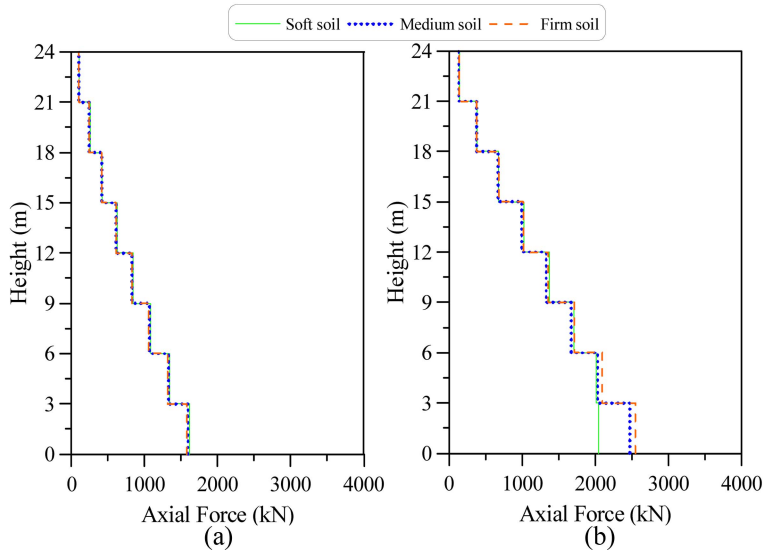


Fig. 24 The site-response effects on the axial force distribution throughout the height of (a) the isolated and (b) the non-isolated buildings

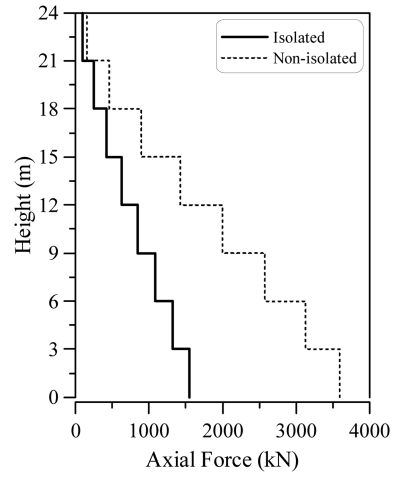


Fig. 25 Axial force distribution throughout the height of the isolated and non-isolated buildings without the site-response effects

Table 8 The mode shapes of the isolated building including site-response effects

Mode No	Soft soil type	Medium soil type	Firm soil type
1			
2			
3			
4			

Table 8 The mode shapes of the isolated building including site-response effects

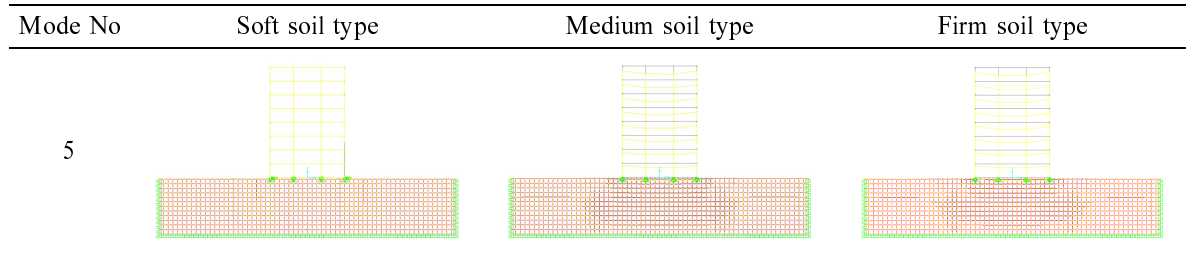
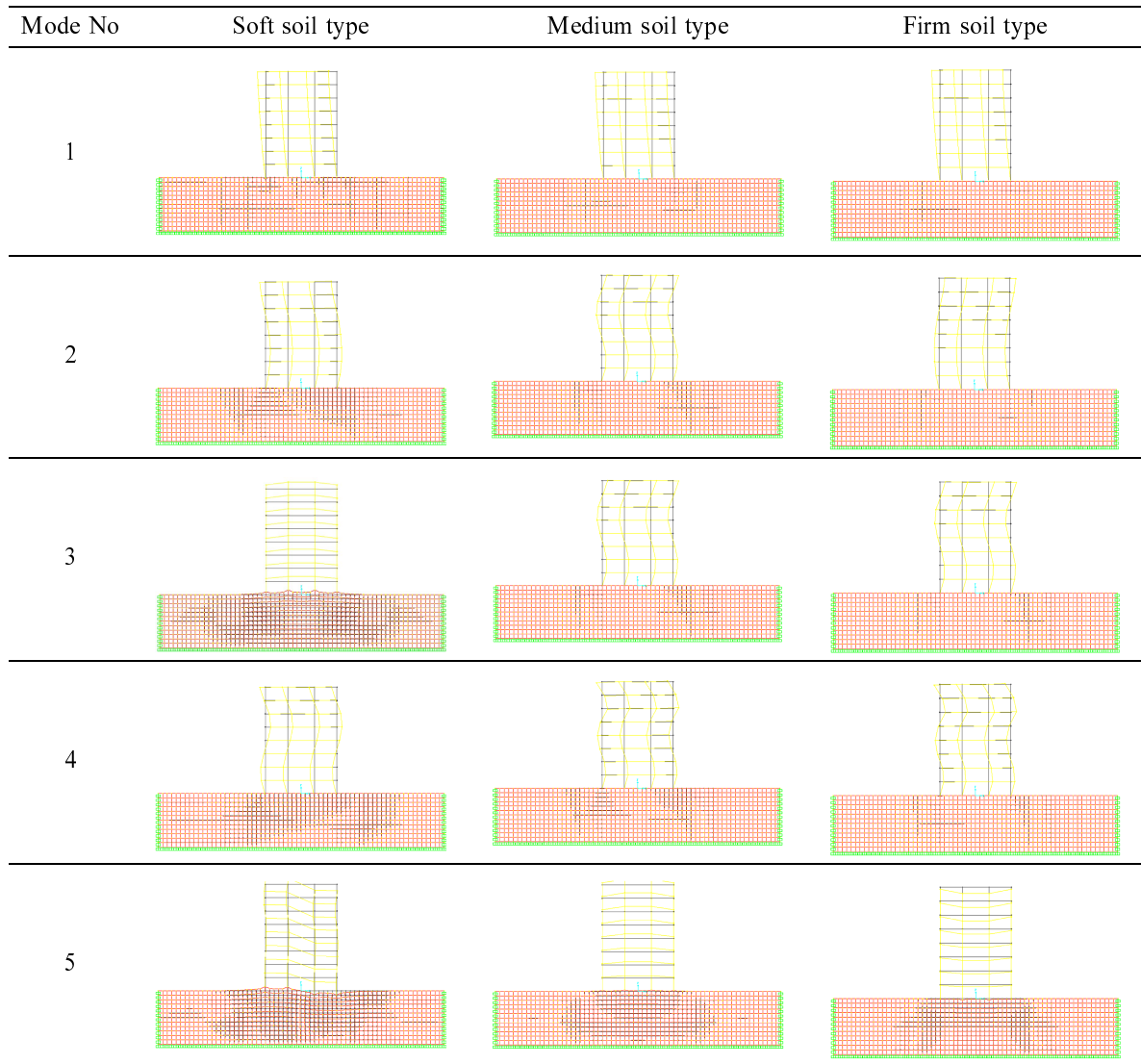


Table 9 The mode shapes of the non-isolated building including site-response effects



building excluding the site-response effects increase. It is stated that inclusion of site-response effect significantly reduces the inertia forces in non-isolated building.

6. Mode shapes

The first five mode shapes for the non-isolated and isolated buildings including site-response effects are provided in Tables 8 and 9, respectively. The periods attained from the analysis are ranging from 0.131 sec to 3.262 sec for the isolated building, and ranging from 0.118 sec to 1.140 sec for non-isolated building as seen in Table 6. The modes shapes are classified as lateral and vertical bending modes.

7. Conclusions

This study provides a new perception on the effect of the seismic isolation on the buildings including the site-response effects. Therefore, a two-dimensional and eight storey of a building with and without isolation system is examined. The triple concave friction pendulum (TCFP) modelled as a series arrangement of the three SCFP bearings is used as a seismic isolation system. The series model is capable of capturing the behaviour of the TCFP bearings. The time history analysis, in order to investigate of the effectiveness of the seismic isolation systems on the buildings, is conducted. It is also considered the site-response effects by finite element method. The non-linear behaviour of the concrete frame is not considered in this study.

Results obtained from the time history analysis were compared with each other. The following results can be obtained from the analyses:

- i. The relative displacements at the each floor of the isolated building with the TCFP bearings are significantly smaller than those of the non-isolated building when the site-response effects are considered.
- ii. The building constructed on the soft foundation soil is more sensitive to ground acceleration as compared to medium and firm foundation soil conditions. The results are viable for both the isolated and the non-isolated buildings. However, the accelerations transmitted to the building decrease by means of using the isolation technique whereas the accelerations increase throughout the floor levels of the non-isolated building.
- iii. The estimation of the displacement capacities of the TCFP bearings is independent of the site-response effects. The displacement capacities of the device does not exceed if the isolated building is constructed on having different stiffness of the foundation soil conditions. On the other hand, the value of capacity of the bearing demanded is viable for soft, medium and firm foundation soil. Furthermore, the possible positions of the TCFP bearings are not change by changing the type of the foundation soils.
- iv. Although inertia forces developed on the columns and beams elements of the non-isolated RC building such as bending moment, shear and axial forces, in case of site-response effect, may substantially decrease as compared to those of the non-isolated building without the site-response effects.
- v. The inertia forces for the isolated RC building disregarding site-response effect do not markedly change with reference to site-response effect is regarded for the isolated RC building.

Finally, the study including site-response effects revealed that seismic isolation systems consisting of the TCFP bearings are considerably effective for the structures constructed on soft, medium and firm soil conditions.

Since the dynamic response of building to earthquake loading is affected by several factors, including intensity and characteristics of the earthquakes, site-response, computer modelling and material properties used in the analysis, the completed responses of the RC building with and without seismic isolation system subjected to Kocaeli earthquake, Turkey, ground motion should not be generalized to usual buildings. Whereas the detailed observations may be dependent on the specific problem, the broad conclusions should apply to many cases.

References

- Akkose, M., Bayraktar, A. and Dumanoglu, A.A. (2008), "Reservoir water level effects on nonlinear dynamic response of arch dams", *J. Fluid Struct.*, **24**, 418-435.
- Ates, S., Soyuluk, K., Dumanoglu, A.A. and Bayraktar, A. (2009), "Earthquake response of isolated cable-stayed bridges under spatially varying ground motions", *Struct. Eng. Mech.*, **31**(6), 639-662.
- Chaudhary, M.T.A., Abe, M. and Fujino, Y. (2001), "Identification of soil-structure interaction effect in base-isolated bridges from earthquake records", *Soil Dyn. Earthq. Eng.*, **21**(8), 713-725.
- Computers and Structures Inc. (2007), *SAP2000: static and dynamic finite element analysis of structures*, Berkeley, CA, U.S.A.
- Constantinou, M.C., Whittaker, A.S., Fenz, D.M. and Apostolakis, G. (2007), "Seismic isolation of bridges", Report submitted to the State of California Department of Transportation.
- Dicleli, M., Albhaisi, S. and Mansour, M.Y. (2005), "Static soil-structure interaction effects in seismic-isolated bridges", *Practice Period. Struct. Des. Constr. - ASCE*, **10**(1), 22-33.
- Fadi, F. and Constantinou, M.C. (2010), "Evaluation of simplified methods of analysis for structures with triple friction pendulum isolators", *Earthq. Eng. Struct. Dyn.*, **39**, 5-22.
- Fenz, D. (2008), "Development, implementation and verification of dynamic analysis models for multi-spherical sliding bearings", PhD. Thesis, The State University of New York at Buffalo.
- Fenz, D.M. and Constantinou, M.C. (2008a), "Development, implementation and verification of dynamic analysis models for multi-spherical sliding bearings", Technical Report MCEER-08-0018, Multidisciplinary Center for Earthquake Engineering Research, University at Buffalo, State University of New York, Buffalo, NY.
- Fenz, D.M. and Constantinou, M.C. (2008b), "Spherical sliding isolation bearings with adaptive behavior: theory", *Earthq. Eng. Struct. Dyn.*, **37**, 163-183.
- Fenz, D.M. and Constantinou, M.C. (2008c), "Modeling triple friction pendulum bearings for response history analysis", *Earthq. Spectra*, **24**, 1011-1028.
- Gazetas, G. (1991), *Foundation vibrations*, Fang HY, editor, Foundation engineering handbook, 2nd ed, (Chapter 15), Chapman & Hall, London.
- Goyal, A. and Chopra, A.K. (1989), "Earthquake analysis of intake-outlet towers including tower-water-foundation-soil interaction", *Earthq. Eng. Struct. Dyn.*, **18**, 325-344.
- Ibrahimbegavich, A. and Wilson, E.L. (1989), "Simple numerical algorithms for the mode superposition analysis of linear structural system with non-proportional damping", *Comput. Struct.*, **33**(2), 523-531.
- Idriss, I.M., Kennedy, R.P., Agrawal, P.K., Hadjian, A.H., Kausel, E. and Lysmer, J. (1979), "Analyses for soil-structure interaction effects for nuclear power plants", *Ad Hoc Group on Soil-Structure Interaction of the Committee on Nuclear Structures and Materials of the Structural Division of ASCE*, New York, NY: ASCE, 978-0-87262-183-1 or 0-87262-183-9.
- Leger, P. and Boughoufalah, M. (1989), "Earthquake input mechanisms for time-domain analysis of dam-foundation systems", *Eng. Struct.*, **11**(1), 37-46.
- Novak, M. and Henderson, P. (1989), "Base-isolated buildings with soil-structure interaction", *Earthq. Eng.*

- Struct. Dyn.*, **18**(6), 751-765.
- Soneji, B.B. and Jangid, R.S. (2008), "Influence of soil-structure interaction on the response of seismically isolated cable-stayed bridge", *Soil Dyn. Earthq. Eng.*, **28**(4), 245-257.
- Spyrakos, C.C. and Beskos, D.E. (1986), "Dynamic response of flexible strip-foundations by boundary and finite elements", *Soil Dyn. Earthq. Eng.*, **5**(2), 84-96.
- Spyrakos, C.C. and Vlassis, A.G. (2002), "Effect of soil-structure interaction on seismically isolated bridges", *J. Earthq. Eng.*, **6**(3), 391-429.
- Spyrakos, C.C., Koutromanos, I.A. and Maniatakis, Ch.A. (2009), "Soil-structure interaction effects on base-isolated buildings including soil-structure interaction", *Soil Dyn. Earthq. Eng.*, **29**, 658-668.
- Tongaonkar, N.P. and Jangid, R.S. (2003), "Seismic response of isolated bridges with soil-structure interaction", *Soil Dyn. Earthq. Eng.*, **23**, 287-302.
- Tsai, C.S., Chen, W.S. and Chiang, T.C. (2010a), "Experimental and numerical studies of trench friction pendulum system", *Struct. Eng. Mech.*, **34**(2), 277-280.
- Tsai, C.S., Lin, Y.C., Chen, W.S., Chiang, T.C. and Chen, B.J. (2010b), "Piecewise exact solution for seismic mitigation analysis of bridges equipped with sliding-type isolators", *Struct. Eng. Mech.*, **35**(2), 205-215.
- Vlassis, A.G. and Spyrakos, C.C. (2001), "Seismically isolated bridge piers on shallow soil stratum with soil-structure interaction", *Comp. Struct.*, **79**(32), 2847-2861.
- Wilson, E.L. (1993), "An efficient computational method for base isolation and energy dissipation analysis of structural systems", ATC-17-1, Applied Technology Council, San Francisco.
- Wolf, J.P. (1985), *Dynamic soil-structure interaction*, Prentice-Hall, New Jersey.
- Wolf, J.P. (1994), *Foundation vibration analysis using simple physical models*, Prentice-Hall, New Jersey.
- Wong, H.L. and Luco, J.E. (1976), "Dynamic response of rigid foundations of arbitrary shape", *Earthq. Eng. Struct. Dyn.*, **4**, 587-597.